Performance analysis for aerial-towing system

IOP Conf. Series: Materials Science and Engineering **610** (2019) 012097 doi:10.1088/1757-899X/610/1/012097

Performance analysis for aerial-towing system

Mostafa Khalil

Aerospace Engineering Department, Military Technical College, Cairo, 11766, Egypt

mostafa.samir@mtc.edu.eg

Abstract. The dynamics of open chain systems have been widely investigated as a result of its increased applications such as aerial towing system, submerged towed cable applications, robot manipulators, and bio-mechanical applications. In this study, a practical engineering system, Mine Clearing Line Charge MICLIC system is taken as an example for an open chain system with accelerated end and varying number of segments. To validate the proposed model, a comparison between two different finite segment methods namely Kane's method and Riccati transfer matrix method of linear multibody system (Riccati-MS-TMM) have been performed for a large open chain system. Results show that computational speed of Riccati-MS-TMM outperforms Kane's method due to its huge matrix size to be solved. Then, using a predefined rocket motor total impulse, a parametric study has been performed on MICLIC system to illustrate the impact of different rocket motor thrust profiles on the resulted flight performance including the missile range, flight time, maximum tension applied on the rocket towing bridle, and the missile stability.

KEYWORDS: finite-segment; MICLIC; open-chain dynamics.

1. Introduction

During past decades, chain dynamics had an important role in mechanical systems design and simulation which has exhaustively investigated through many researchers from literature. This problem was first illustrated by Mcleod [1]. However no numerical solutions were attempt for general usage, the aerodynamic lift and drag loads on aerial towed cables due to wind was illustrated regardless the applied gravitational load. Gluart [2] developed a family of curves to obtain cable parameters for a given weight-drag ratio. An approximate analytical formula has been presented [3] to compute cable shape and tension applied for non-accelerated case. Numerous mathematical models from literature have been developed to simulate the open chain problem based on different numerical techniques which are good presented by Zhu and Meguid [4]such as, finite-difference approximation [5-8] , finite-segment method [9-14], and

finite-element method [4, 15, 16]. Due to its simplicity, finite difference approximation has been widely used in literature to solve open chain problem dynamics under the assumption of invariant chain properties along its length.

Based on finite-segment method, number of studies were devoted to investigate the dynamics of aerial refueling system including tanker's storage pod, a refueling hose, and the drogue. Ro and Kamman[9] developed a model to simulate the motion of tanker hose-drouge assembly in the presence of atmospheric turbulence. The hose was segmented into 20-lumped mass with ball-and-socket rigid links, which subjected to gravitational and aerodynamic forces. By computing the accelerations for each adjacent lumped masses, the corresponding link tension can be obtained. In order to capture the phenomena of hose whipping motion in absence of reel motion, Ribbens et al.[10] developed a dynamic model for an aerial refueling system. The hose has been segmented into 10 nodes of lumped masses with massless nonlinear spring link between each successive nodes. In addition to the action of gravitational and aerodynamic loads on the hose, hose bending stiffness was included based on standard beam bending theory. The flight refueling system performance has been investigated [17, 18] based on different flight scenarios to illustrate the impact of reel system malfunctions on hose-whip problem. A transfer matrix method of linear multibody system MS-TMM has been developed by Rui et.al. [19] to study the dynamics of multi-body systems. Due to the accumulated error arises through huge chain multi-rigid-body system, a new form named as Riccati-MS-TMM has been proposed [20] by combining Riccati transform [21] with MS-TMM to reduce the order of utilized matrices in MS-TMM and hence improve the system effectiveness and corresponding computational time.

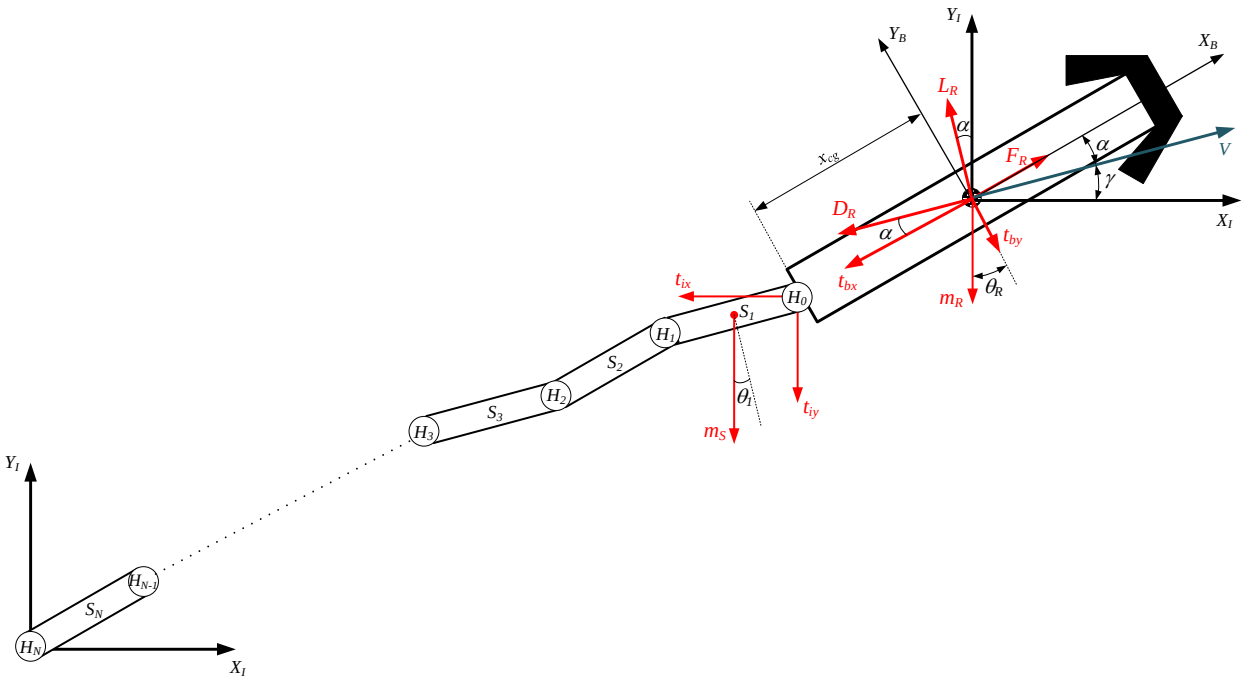

Fig. 1 Topology figure for MICLIC system dynamics model

Mine Clearing Line Charge MICLIC system is one of the open chain aerial towed applications, which is used against various minefields including anti-armor, vehicles and personnel consisting of rocket motor, towing bridle, explosive line charge, safety and arming fuze, and connected chassis. Limited number of studies from literature have been proposed [13, 22]. In this paper, a comparison between traditional Kane's method and Riccati-MS-TMM for a huge chain system has been performed.

2. Mathematical Model

Normally, the missile airframe needs to retain proper value for in-flight stability to ensure that its mission is reached. This criteria can be achieved by using fin-stabilized or spin-stabilized means. In MICLIC system, only a rocket motor without any kind of stability is utilized to obtain the impulse required to pull the explosive line charge to a desired ground range. However, the rocket motor achieves its in-flight stability by means of varied continuous tension resulted from the explosive line charge over flight trajectory. In this paper, MICLIC system has been modeled as multi-rigid-body connected by frictionless hinges. As illustrated in Fig. 1, the rocket motor *R* is regarded as a rigid-body following the pitch three-degree-of-freedom equations of motion [23] mounted to the accelerated end of the explosive line charge. The explosive line charge is divided into *N* chain segments regarded as a rigid-body, their sequence numbers are S_1, S_2… S_N. These chain segments are connected together by means of weightless joints regarded as *N+1* smooth-ball-and-socket hinge, whose sequence numbers are H_0, H_1, H_2… H_N, where H_0 is the accelerated end of the explosive line charge while H_N is the ground fixed end. The motion of the proposed system is assumed to be in vertical plane (X_I, Y_I) as the impact of cross-wind has been neglected.

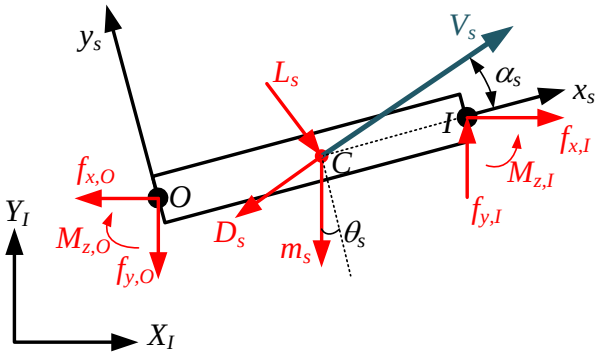

Fig. 2 Forces and moments applied on chain segment with input *I* and output *O* in plane

2.1. Missile Flight Model

The missile three-degree-of-freedom equations of motion[23] has been implemented, which describes its motion in the vertical plane (X_I, Y_I) as an inertial coordinates which has been located at the launch site on ground level as mentioned in Fig. 1. Considering the missile is affected by aerodynamic drag $D_R = q_R C_D S_R$, lift $L_R = q_R C_L S_R$, and pitching moment $M_R = q_R C_m S_R d_R$, motor thrust *F*, gravitational acceleration *g*, and the explosive line tension applied on the rocket base $T = [t_{bx} \quad t_{by}]^T$, the missile equations of motion are stated as,

$$m_R\dot{V}_R = F\cos\alpha - m_R g\sin\gamma - D_R - t_{bx}\cos\alpha + t_{by}\sin\alpha \quad (1)$$

$$m_R V_R\dot{\gamma} = F\sin\alpha - m_R g\cos\gamma + L_R - t_{bx}\sin\alpha - t_{by}\cos\alpha \quad (2)$$

$$J_R\ddot{\theta} = M_R + t_y^b.x_{cg} \quad (3)$$

where, $V = \sqrt{{V_X}^2 + V_y^2}$ is the missile total velocity, m is the missile mass, x_{cg} is the missile center of gravity measured from missile base, J_R is the missile lateral moment of inertia computed at mass center, α is the missile angle of attack, $q_R = 0.5\,\rho\,V_R^2$is the missile dynamic pressure, C_D, C_L, and C_m are the missile aerodynamic drag, lift, and moment coefficients respectively, γ is the missile flight path angle, and θ is the missile pitch angle. The transformation matrix to transfer any given vector from inertial frame (X_I, Y_I) to body fixed frame (X_B, Y_B) as illustrated in Fig. 1 is given by

$$A = \begin{bmatrix} \cos\theta & \sin\theta \\ -\sin\theta & \cos\theta \end{bmatrix} \quad (4)$$

2.2. Explosive line charge

The hose is divided into *N* rigid segments connected by *N+1* weightless smooth ball-and-socket hinges as shown in Fig. 1. Each segment has a length l_s, mass m_s, and lateral moment of inertia J_s at input point *I*. Based on transfer matrix method of multibody system MS-TMM [20], The state vectors of the connection point among each body/hinge moving in plane is defined as

$$Z = [\,\ddot{x} \quad \ddot{y} \quad \ddot{\theta} \quad M_z \quad f_x \quad f_y \quad 1]^T \quad (5)$$

where, $\ddot{x}$ and $\ddot{y}$ are the connection point linear acceleration in x and y directions respectively, $\ddot{\theta}$ is the angular acceleration for body/hinge connection point, and M_z, f_x, and f_y are the moment and forces between any two successive elements. The transfer equation that describe the motion of one point to another is given by,

$$Z_{i+1} = U_i Z_i \quad (6)$$

where, U_i is the transfer matrix that summarizes all motion characteristics of such element which will be illustrated as [20, 24],

2.2.1. Transfer matrix of rigid-body moving in plane. To determine the chain segment transfer matrix, let (X_I, Y_I) be the inertial frame located at the launch site on ground level as mentioned in Fig. 2, ($X_{c,n}$, $Y_{c,n}$) be the local body frame located at the mass center *C* of current *n* segment, points *I* and *O* represents the input and output points respectively. The chain segment is moving under the action of aerodynamic forces and gravity illustrated in Fig. 2 as, $[f_{xC} \quad f_{yC}]^T = A^T.[D_s \quad L_s]^T$where, $D_s$and L_s are the applied aerodynamic drag and lift forces applied on the chain segment to be calculated as presented in [13]. Based on the

equations of motion of rigid body deduced in [20, 24], the transfer matrix of a uniform chain segment U_s is given by,

$$U_{s,n} = \begin{bmatrix} 1 & 0 & -y_{IO} & 0 & 0 & 0 & -x_{IO}\dot{\theta}_{s,n} \\ 0 & 1 & x_{IO} & 0 & 0 & 0 & -y_{IO}\dot{\theta}_{s,n} \\ 0 & 0 & 1 & 0 & 0 & 0 & 0 \\ -y_{OC}m_{s,n} & x_{OC}m_{s,n} & u_{4,3} & 1 & -y_{IO} & x_{IO} & u_{4,7} \\ -m_{s,n} & 0 & y_{IC}m_{s,n} & 0 & 1 & 0 & u_{5,7} \\ 0 & -m_{s,n} & -x_{IC}m_{s,n} & 0 & 0 & 1 & u_{6,7} \\ 0 & 0 & 0 & 0 & 0 & 0 & 1 \end{bmatrix} \quad (7)$$

where,

$[x_{IO} \quad y_{IO}]^T = A^T.[-l_s \quad 0]^T$, $[x_{IC} \quad y_{IC}]^T = A^T.[-l_s/2 \quad 0]^T$, $u_{5,7} = f_{xC} + m_{s,n}\dot{\theta}_{s,n}^2 x_{IC}$, $u_{4,3} = J_s - m_{s,n}(x_{IO}x_{IC} + y_{IO}y_{IC})$, $[x_{OC} \quad y_{OC}]^T = [x_{IC} - x_{IO} \quad y_{IC} - y_{IO}]^T$, $u_{6,7} = f_{yC} + m_{s,n}\dot{\theta}_{s,n}^2 y_{IC}$, $u_{4,7} = m_{s,n}\dot{\theta}_{s,n}^2(x_{IO}y_{IC} - y_{IO}x_{IC}) + (y_{OC}f_{xC} - x_{OC}f_{yC})$.

2.2.2. Transfer matrix of smooth-ball-and-socket hinge moving in plane. By neglecting its mass and size, and considering that all internal forces and coordinates are equal while no internal moments are applied through both ends, then the transfer matrix of the hinge between any two successive chain segments is given by [20, 24],

$$U_{h,n} = \begin{bmatrix} 1 & 0 & 0 & 0 & 0 & 0 & 0 \\ 0 & 1 & 0 & 0 & 0 & 0 & 0 \\ \frac{y_{OC}m_{s,n}}{u_{4,3}} & \frac{-x_{OC}m_{s,n}}{u_{4,3}} & 0 & \frac{y_{IO}}{u_{4,3}} & \frac{-x_{IO}}{u_{4,3}} & 0 & \frac{u_{4,7}}{u_{4,3}} \\ 0 & 0 & 0 & 1 & 0 & 0 & 0 \\ 0 & 0 & 0 & 0 & 1 & 0 & 0 \\ 0 & 0 & 0 & 0 & 0 & 1 & 0 \\ 0 & 0 & 0 & 0 & 0 & 0 & 1 \end{bmatrix} \quad (8)$$

3. Results and discussion

3.1. Model Validation

In order to validate the proposed model, a simulation for huge chain multi-rigid body system is implemented containing up to 200 segments with equal mass 1 kg and length 1 m, where the aerodynamic forces has been neglected. The boundary conditions applied at both fixed and free-ends are $[0 \quad 0 \quad \ddot{\theta} \quad 0 \quad f_x \quad f_y \quad 1]^T$, $[\ddot{x} \quad \ddot{y} \quad \ddot{\theta} \quad 0 \quad 0 \quad 0 \quad 1]^T$ respectively.

The results obtained are compared with the one obtained from Kane's method with lumped-mass approximation as proposed in [13]. Runge-kutta-4 with fixed time step 0.001 s are utilized for both methods. In case of Kane's method, as the system degrees of freedom increases, the dimension of matrices that represents system dynamics also increased. However, Riccati-MS-TMM keeps the same system matrices size regardless system complexity as illustrated in Fig. 3. For example, a numerical simulation for *N*=١٠٠ chain size is performed. As illustrated in Fig. 4, a comparison between the computed angular displacement of segment number 1 and

50 at the root and middle of the chain respectively is done based on the methods listed above. It can be concluded that Riccati-MS-TMM outperforms Kane's method in both accuracy and computation time.

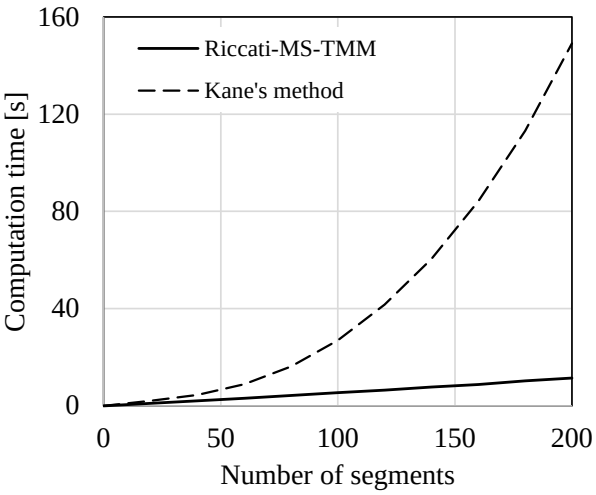

Fig. 3 Computational time vs. chain segments number

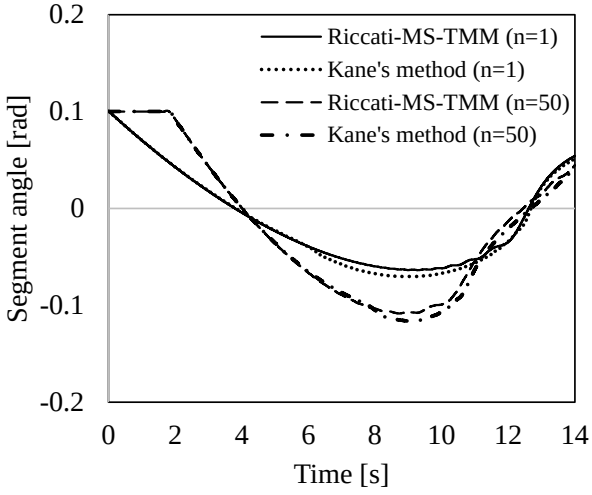

Fig. 4 Displacement angles for segments no.1 and 50 for chain with N = 100

3.2. Problem description

As a realistic engineering problem, Mine Charge Line Cleaning MICLIC system is presented to investigate the impact of different rocket motor thrust-profiles including, neutral, dual, regressive, and progressive-burning on the system flight performance. All these four scenarios are assumed to have constant total impulse 20 kN.s and burning time 2 s as listed in Table ١.

The rocket motor is launched with 5 m/s initial velocity with 35° elevation angle which corresponds to maximum allowable range as concluded in [13].As illustrated in Fig. 1, the rocket motor initial mass is 60 kg including 15 kg propellant. The explosive line consists of 100 m of high explosive with mass 7 kg/m, and 50 m of rope with mass 0.5kg/m including 150 rigid-body with 151 weightless smooth-ball-and-socket hinges. The hinge H_0 is connected to the base of the rocket as a moving end with boundary condition $[\ddot{x}_R \quad \ddot{y}_R \quad \ddot{\theta} \quad 0 \quad t_{ix} \quad t_{iy} \quad 1]^T$, where $\ddot{x}_R$ and $\ddot{y}_R$ are the computed rocket acceleration through flight time. The other end is freely to move pulling a new segment under the condition of $[\ddot{x} \quad \ddot{y} \quad \ddot{\theta} \quad 0 \quad f_x \quad f_y \quad 1]^T$, where the problem of hinge reactions f_x and f_y at last segment are simplified using the model proposed in [25].

3.3. Results

For all numerical simulations listed in Table ١, the Runge-kutta-4 with fixed time step 0.001 s are utilized. As shown in Fig. 5, the angle of attack AOA for different case studies are illustrated through active motor phase. The initial motor thrust value has a significant impact on the rocket AOA and hence its stability during its initial flight. As the initial motor thrust increases, the rocket flight will be more stable.

From experience gained from field experiment, accidents may occur such as rocket tumbling if the motor didn't give the proper thrust. In addition, sudden changes in rocket thrust results in sudden increase in the tension force applied on the rocket base as in case-2 illustrated in Fig. 6. So it's better to use motor with neutral burning or gradually change the motor thrust through powered phase as progressive, and regressive burning cases. Fig. 7 illustrates a comparison between the rocket flight paths for different motor cases. As the rocket motor end after 2 s, the number of explosive line segments pulled by different motor cases are 98, 96, 93, and 103 respectively. As the rocket pulled the whole explosive line (i.e. 150 segments), the corresponding flight time and rocket normal velocity are (3.39s, −1.89m/s), (3.47s, −1.95m/s), (3.55s, −3.86m/s), and (3.24s, 0.31m/s) respectively. Hence, case-4 namely the regressive burning motor case outperforms other motor cases.

A further comparison between dual-thrust motor and regressive burning cases is implemented in terms of explosive line tensile force *T*, rocket velocity, and line instantaneous end acceleration $\ddot{y}$. As shown in Fig. 8, the tension force applied to rocket base suddenly increased from approximately 5kN to 15kN as a result of transient phase for dual-thrust case at time 0.75s, while the tensile load almost stable with approximately 7 kN average value in case of regressive-burning. As a result the high propulsive force applied initially through launching phase, the rocket can pull the explosive line away in shorter time compared to case-2 by reducing the energy loss due to the tensile effect as shown in Fig. 9. On the other hand, as mentioned in Fig. 10, the explosive line experienced a high accelerations in the contact point between temporally last pulled segment and the charge stack during the pulling process, which may cause the explosive line external fabric material to fracture during the process of pulling from its storage box. In case-4, with the exception of the initial pulling acceleration, a smooth change is obtained other than the sharp changes experienced through case-2.

Table 1 Thrust profiles for suggested scenarios

Case #	Rocket Motor	T(t) [kN]		Propellant burning rate [kg/s]	
1	Neutral burning	10		7.5	
2	Dual thrust	8	$(0.00 \le t < 0.75)$	6	$(0.00 \le t < 0.75)$
		16	$(0.75 \le t < 1.25)$	12	$(0.75 \le t < 1.25)$
		8	$(1.25 \le t < 2.00)$	6	$(1.25 \le t < 2.00)$
3	Progressive burning	8 + 2 t		6 + 0.75 t	
4	Regressive burning	12 – 2 t		9 – 0.75 t	

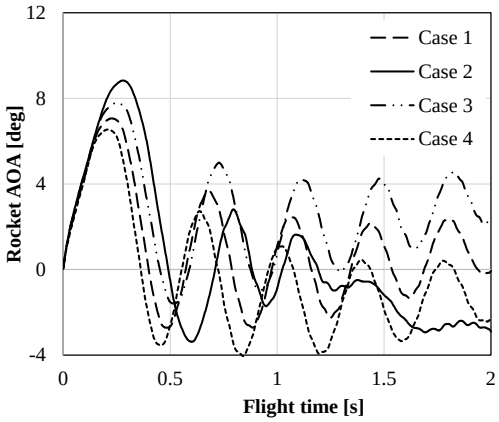

Fig. 5 The rocket AOA for powered phase

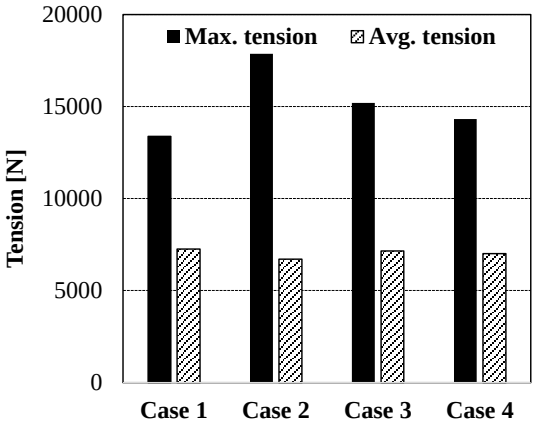

Fig. 6 The tension force applied on rocket base

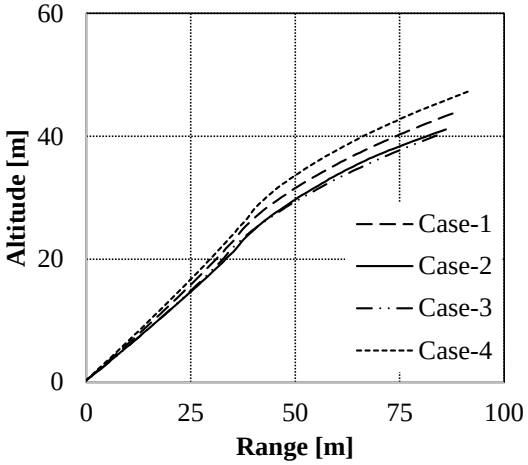

(a) t = 2 s

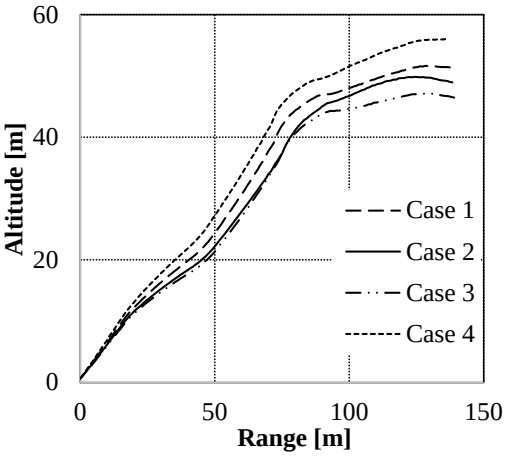

(b) End of line charge N = 150

Fig. 7 The rocket flight path for different motor cases

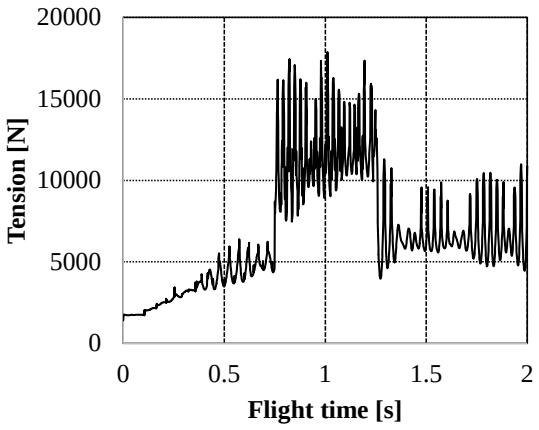

(a) Case-2

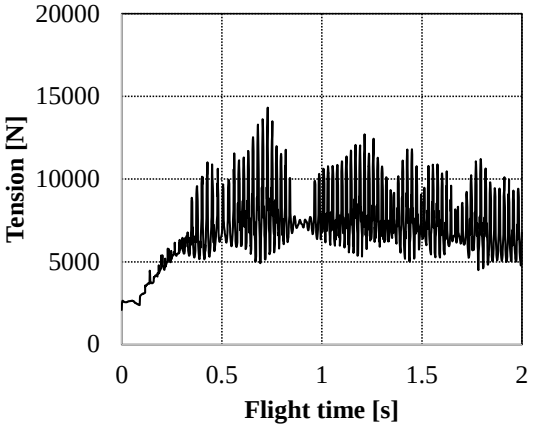

(b) Case-4

Fig. 8 Tension force applied on the rocket base through powered phase for cases 2 and 4

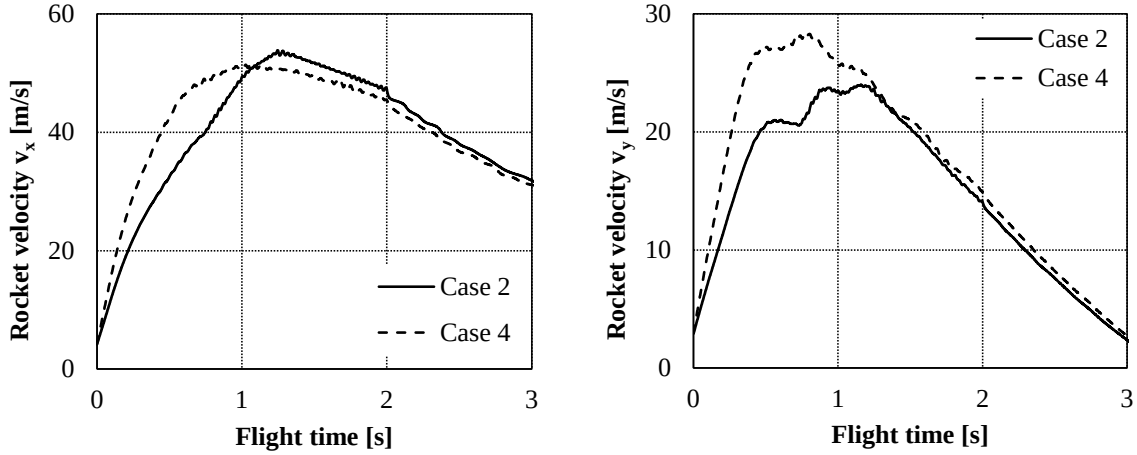

(a) axial velocity (b) normal velocity

Fig. 9 The rocket velocity components for cases 2 and 4

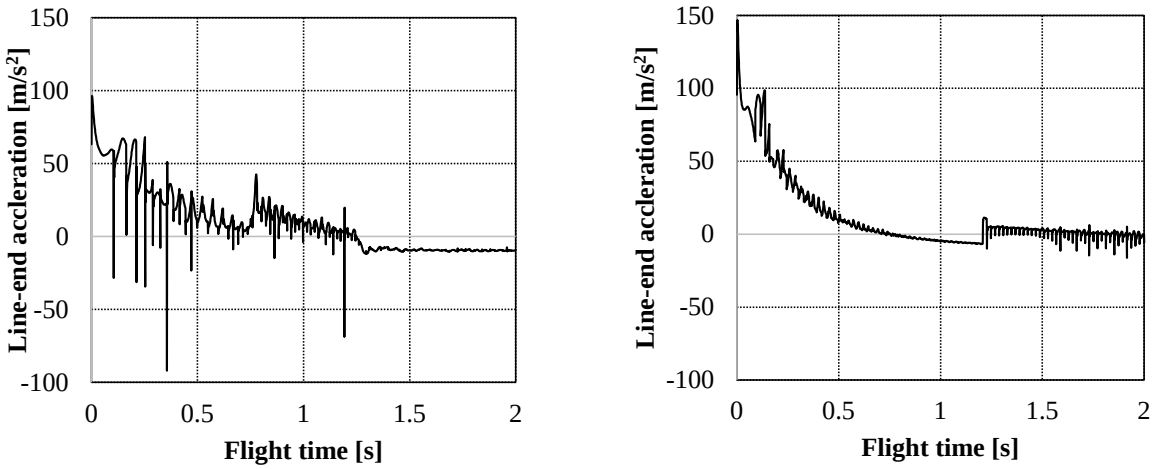

(a) Case-2 (b) Case-4

Fig. 10 The acceleration of the point between temporally last pulled segment and explosive charge stack for cases 2 and 4

4. Conclusion

In this paper, a numerical model has been developed to simulate the flight path of Mine Clearing Line Charge MICLIC system containing the rocket motor and the explosive line charge. This system is considered as an open chain system with accelerated end (i.e. rocket motor) and varying number of segments (i.e. explosive line) including 150 rigid-body with 151 weightless smooth-ball-and-socket hinges. The formulation of the proposed method namely Riccati-MS-TMM method for chain moving in plane has been illustrated. A comparison has been done to show the computational time efficiency for the proposed method relative to traditional Kane's method from literature. A parametric study has been performed to show the impact of different thrust-profiles on the system performance as, (1) the rocket tumbling especially after launch, can be reduced using proper thrust based on charge weight-per-unit-length, (2) sudden changes in motor thrust may cause extreme tension load on the connecting wire between rocket and explosive charge which may cause wire fracture, and (3)

explosive charge line experienced high accelerations and hence high loads at some locations which may cause fracture for charge line external fabric material.

References

[1] McLeod A 1919 *On the Action of Wind on Flexible Cables, with Applications to Cables Towed Below Aeroplanes, and Balloon Cables*: HM Stationery Office)
[2] GLAUERT H 1934 The form of a heavy flexible cable used for towing a heavy body below an aeroplane. Advisory Committe for Aeronautics *Reports and Memoranda* 1108-22
[3] Narkis Y 1977 Approximate solution for the shape of flexible towing cables *Journal of Aircraft* **14** 923-5
[4] Zhu Z H and Meguid S A 2006 Elastodynamic analysis of aerial refueling hose using curved beam element *AIAA journal* **44** 1317-24
[5] Ablow C and Schechter S 1983 Numerical simulation of undersea cable dynamics *Ocean engineering* **10** 443-57
[6] Mehrabi A B and Tabatabai H 1998 Unified finite difference formulation for free vibration of cables *Journal of Structural Engineering* **124** 1313-22
[7] Koh C, Zhang Y and Quek S 1999 Low-tension cable dynamics: Numerical and experimental studies *Journal of Engineering Mechanics* **125** 347-54
[8] Wu Q, Takahashi K and Nakamura S 2003 Non-linear vibrations of cables considering loosening *Journal of Sound and Vibration* **261** 385-402
[9] Ro K and Kamman J W 2010 Modeling and simulation of hose-paradrogue aerial refueling systems *Journal of guidance, control, and dynamics* **33** 53-63
[10] Ribbens W, Saggio F, Wierenga R and Feldmann M 2007 Dynamic modeling of an aerial refueling hose & drogue system. In: *25th AIAA Applied Aerodynamics Conference*, p 3802
[11] Winget J and Huston R 1976 Cable dynamics—a finite segment approach *Computers & Structures* **6** 475-80
[12] Huston R L and Kamman J W 1982 Validation of finite segment cable models *Computers & Structures* **15** 653-60
[13] Gu W-b, Lu M, Liu J-q, Dong Q-x, Wang Z-x and Chen J-h 2014 Simulation and experimental research on line throwing rocket with flight *Defence Technology* **10** 149-53
[14] Pandy M G and Berme N 1988 A numerical method for simulating the dynamics of human walking *Journal of biomechanics* **21** 1043-51
[15] Styuart A, Gaston R, Yamashiro H, Stirling R and Mor M 2011 Numerical simulation of hose whip phenomenon in aerial refueling. In: *AIAA Atmospheric Flight Mechanics Conference*, p 6211
[16] Zhu Z and Meguid S 2007 Modeling and simulation of aerial refueling by finite element method *International Journal of Solids and Structures* **44** 8057-73
[17] Vassberg J, Yeh D, Blair A and Evert J 2004 Numerical simulations of KC-10 centerline aerial refueling hose-drogue dynamics with a reel take-up system. In: *22nd Applied Aerodynamics Conference and Exhibit*, p 4719
[18] Vassberg J, Yeh D, Blair A and Evert J 2003 Numerical simulations of KC-10 wing-mount aerial refueling hose-drogue dynamics with a reel take-up system. In: *21st AIAA Applied Aerodynamics Conference*, p 3508

[19] Rui X, Wang G, Lu Y and Yun L 2008 Transfer matrix method for linear multibody system *Multibody System Dynamics* **19** 179-207
[20] Rui X, Wang G and Zhang J 2018 *Transfer Matrix Method for Multibody Systems: Theory and Applications*: Wiley)
[21] Horner G C and Pilkey W D 1978 The Riccati transfer matrix method *Journal of Mechanical Design* **100** 297-302
[22] Han F, Chen H and Zhu Q 2013 Modelling and simulation of a rocket-towed net system *International Journal of Modelling, Identification and Control* **20** 279-85
[23] Jackson P B 2010 Overview of missile flight control systems *Johns Hopkins APL technical digest* **29** 9-24
[24] Rui X, Bestle D, Zhang J and Zhou Q 2016 A new version of transfer matrix method for multibody systems *Multibody System Dynamics* **38** 137-56
[25] Wolf D 1971 Dynamic stability of a nonrigid parachute and payload system *Journal of Aircraft* **8** 603-9